

Article

Antibacterial Efficiency of Stainless-Steel Grids Coated with Cu-Ag by Thermionic Vacuum Arc Method

P. Dinca^{1,2}, B. Butoi^{1,2}, M. Lungu^{1,2}, C. Porosnicu^{1,*}, I. Jecu¹, C. Staicu^{1,2}, C.P. Lungu¹, A. Niculescu^{1,3}, I. Burducea⁴ , O. Trusca⁵, M. Diaconu⁶, I. Cretescu⁶ and G. Soreanu⁶

¹ National Institute for Laser, Plasma and Radiation Physics, 409 Atomistilor Street, 077125 Magurele, Romania; paul.dinca@inflpr.ro (P.D.); bogdan.butoi@inflpr.ro (B.B.); mihail.lungu@inflpr.ro (M.L.); ionut.jecu@inflpr.ro (I.J.); cornel.staicu@inflpr.ro (C.S.); cristian.lungu@inflpr.ro (C.P.L.); ana.niculescu@inflpr.ro (A.N.)

² Faculty of Physics, University of Bucharest, 405 Atomistilor Street, 077125 Magurele, Romania

³ Faculty of Mathematics and Natural Sciences, University of Craiova, RO-200585 Craiova, Romania

⁴ Horia Hulubei National Institute of Physics and Nuclear Engineering, 077125 Magurele, Romania; bion@nipne.ro

⁵ Ion Mincu University of Architecture and Urbanism, 010014 Bucharest, Romania; otrusca@yahoo.com

⁶ Gheorghe Asachi Technical University of Iasi, Department of Environmental Engineering and Management, 700050 Iasi, Romania; mdiaconu@tuiasi.ro (M.D.); icre@tuiasi.ro (I.C.); gsor@tuiasi.ro (G.S.)

* Correspondence: corneliu.porosnicu@inflpr.ro

Received: 31 January 2020; Accepted: 23 March 2020; Published: 28 March 2020



Abstract: Autonomous smart natural ventilation systems (SVS) attached to the glass façade of living quarters and office buildings can help reducing the carbon footprint of city buildings in the future, especially during warm seasons and can represent an alternative to the conventional mechanical ventilation systems. The work performed in this manuscript focuses on the investigation of bacteria trapping and killing efficiency of stainless steel grids coated with a mixed layer of Cu-Ag. These grids are to be employed as decontamination filters for a smart natural ventilation prototype that we are currently building in our laboratory. The tested grids were coated with a mixed Cu-Ag layer using thermionic vacuum arc plasma processing technology. The fixed deposition geometry allowed the variation of Cu and Ag atomic concentration in coated layers as a function of substrate position in relation to plasma sources. The test conducted with air contaminated with a pathogen strain of *staphylococcus aureus* indicated that the filtering efficiency is influenced by two parameters: the pore size dimension and the coating layer composition. The results show that the highest filtering efficiency of 100% was obtained for fine pore (0.5 × 0.5 mm) grids coated with a mixed metallic layer composed of 65 at% Cu and 35 at% Ag. The second test performed only on reference grids and Cu-Ag (65–35 at%) under working conditions, confirm a similar filtering efficiency for the relevant microbiological markers. This particular sample was investigated from morphological, structural, and compositional point of view. The results show that the layer has a high surface roughness with good wear resistance and adhesion to the substrate. The depth profiles presented a uniform composition of Cu and Ag in the layer with small variations caused by changes in deposition rates during the coating process. Identification of the two metallic phases of the Cu and Ag in the layers evidences their crystalline nature. The calculated grain size of the nanocrystalline was in the range 14–21 nm.

Keywords: Cu-Ag layers; coated grids; bacteria; antibacterial efficiency; air filtering

1. Introduction

The air has an extremely important epidemiological role, representing a way of transmission for a large number of pathogens. The infectious diseases caused by air-carried pathogens have the highest occurrence rate, at least on temperate areas of the planet, and represents a percentage of almost 20% of infectious diseases. Individuals in large urban agglomerations have a tendency to spend most of their time indoors. In this context ventilating and air conditioner systems are essential to create and provide stable and comfortable climate conditions in confined spaces especially in homes, offices, schools, hospitals, and other public buildings. In order to avoid circulating large volumes of air contaminated with micro-organisms indoors these installations require efficient air filtering solutions. However, in particular because of moisture and poor maintenance, conventional air filters tend to become fertile breeding surfaces for microbes and bacteria, resulting in biologically contaminated low-quality indoor air that can affect the population health [1].

One of the most common pathogenic agents responsible for bacterial infections is *Staphylococci aureus*. Staphylococci are part of the Micrococcaceae family. There are 27 species and 7 subspecies and only 3 of them represent a bacteriological interest: *S. aureus*, *S. epidermidis*, and *S. saprophyticus*. Staphylococci colonize preponderantly on the superior airways [2] and the skin surface [3,4]. Most strains are not pathogenic, a part of them are conditional and a few are pathogenic. Their resistance in external environment (in the air) is relatively high, thus being the reason why they constantly contaminate human environment [5,6]. *S. aureus* is a conditioned pathogen, so it generates infections crossing barriers of natural defense and the immunity response is inefficient [7–9]. Primary habitat of staphylococcus consists of skin and mucous, where staphylococci are then circulated directly by the hands or indirectly through the dust to people susceptible to infection [5,10–12]. Both copper (Cu) and silver (Ag), which are the selected elements for this study, are well-known since the ancient times because of their natural antibacterial properties [13,14]. Lately, because of increased resistance of bacteria to antibiotics, Cu and Ag have been brought again into attention as a prevention mechanism due to their rapid killing bacteria properties [15]. Also, because of their outstanding broad spectrum antimicrobial activity against a large variety of fungi, viruses, and bacteria these metallic agents are considered promising as an efficient modern approach to the air filtration problem in [16–18]. Another advantage is represented by the fact that this material can be easily attached to the conventional air filtering systems (metallic grids, textile filters or HEPA filters) reducing the number of micro-organisms [1]. Large-scale implementation as bactericidal surfaces composed of these two materials is largely prevented because of the relatively high costs of bulk materials. This problem can be solved by plasma processing technologies which have the potential to cover large surfaces with thin layers (micro or nano scale) using a reduced amount of material.

In this study we focused on developing the air filtration module for the SVS prototype that we are currently constructing. One of the obvious weaknesses of natural ventilation systems compared to mechanical ventilation is represented by air filtering. For mechanical ventilation high retention efficiency textile and HEPA filters can be employed to filter small particles, volatile compounds, and micro-organisms from intake air. Since natural ventilation rely on air currents flow from outdoor to indoor, the mentioned filters cannot be mounted on natural ventilation systems because of the fact that they will obviously restrict air flow into the buildings. In the current work we explore the possibility of employing Cu-Ag coated stainless steel grids into the air filtration module, considering that based on airflow simulation we conducted previously we determined that both pores dimension (1×1 mm and 0.5×0.5 mm) of the employed grids have no significant influence on air intake volume. The stainless-steel grids were coated using thermionic vacuum arc method (TVA) with a Cu-Ag layers with various atomic ratios to asses which layer composition presents the best antibacterial properties. The main challenge is to find the best combination in terms of layer composition and pore size dimension to obtain the maximum micro-organism filtration efficiency. The first test to evaluate bacterial retention and bactericidal properties consisted in exposing the Cu-Ag-coated grids to air flows contaminated with a common *S. aureus* pathological strain. The second test consisted in exposing

the coating, which showed the best results in the first test, to atmospheric outdoor air under normal working conditions.

2. Materials and Methods

2.1. Thin films Coating Method

Silver and copper antibacterial coatings were obtained by using thermionic vacuum arc method. The working principle of TVA technology was thoroughly described in a series of studies [19–22].

To investigate the antibacterial properties of Cu-Ag used in air filtration, these type of layers were deposited on fine (0.5×0.5 mm pores) and coarse mesh grids (1×1 mm pores), with the metallic thread diameter of $200 \mu\text{m}$. In a separate deposition batch mirror-polished silicon substrates 12×15 mm and 25 mm diameter stainless steel disks were coated in order to perform structural and morphological and compositional analysis on them. A list of measurements performed on each deposited type of substrates is presented in Table 1.

Table 1. Measurements performed on each substrate type coated with Cu-Ag.

Sample Type	Measurements
Cu-Ag layers deposited on air filtration coarse and fine mesh grids	<ol style="list-style-type: none"> 1. Antibacterial testing with <i>S. aureus</i> bacterial strain 2. Outdoor air filtration measurements 3. X-ray fluorescence
Cu-Ag layers deposited on silicon substrates	<ol style="list-style-type: none"> 1. X-ray diffraction 2. Rutherford backscattering spectrometry
Cu-Ag layers deposited on stainless steel disks	<ol style="list-style-type: none"> 1. Tribo-measurements 2. Atomic force microscopy and scanning electron microscopy

The substrates were ultrasonically cleaned and placed on a holder inside the vacuum vessel. One with the silicon and stainless-steel disks and the other with the grids used for antibacterial testing. In order to obtain high purity coating the reaction chamber was heated at $400 \text{ }^\circ\text{C}$ and outgassed prior to the deposition process. After this procedure, high vacuum conditions were obtained (5×10^{-6} torr). Two TVA anode–cathode systems were used as plasma sources for deposition (Figure 1).

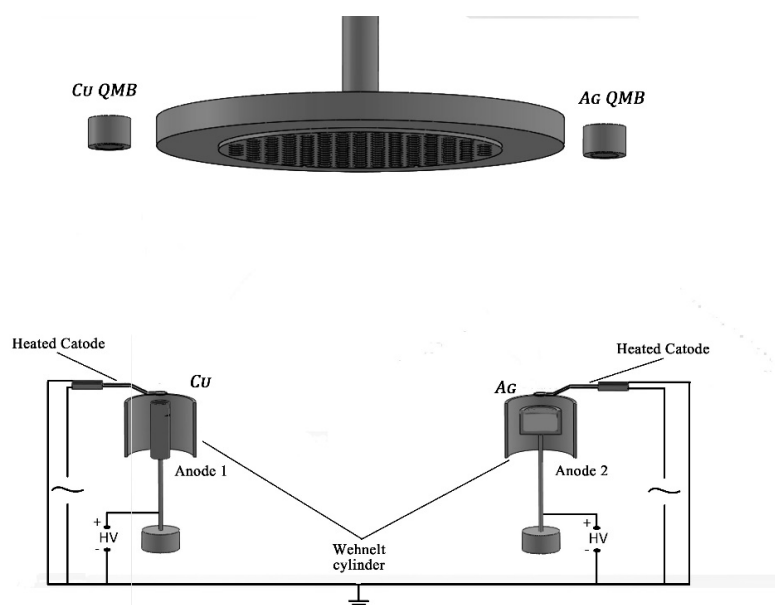


Figure 1. Experimental set-up for Cu-Ag antibacterial coatings.

The high purity (99.95%) materials Ag and Cu, that represents the anodes of the discharge, were placed in two separate TiB_2 crucibles which have a higher melting point than both materials used for the deposition. During the coating procedure, the pressure in the reaction chamber was maintained stable in order to avoid gas inclusion in the samples. Both Cu and Ag anodes were water-cooled during the mixed layers deposition to protect the vacuum chamber gaskets. As illustrated in Figure 1 the cathodes are made of tungsten wire 1 mm in diameter with a loop above the anode with a diameter of 5 mm. To achieve a stable electron thermo-emission the cathodes are heated by passing a high current (30–60 A) from external DC power supply. It is also important to mention that after the outgassing procedure Ar gas was fed into the vacuum chamber in a controlled manner through a mass flow device and a discharge was ignited on the substrates to remove surface impurities and improve layer bonding. During deposition the cathodes were operated using a 42 A current for Cu and 39 A for Ag. The thermo-emitted cathode electrons were accelerated toward the anodes by applying potential difference of 650 V on Cu anode and 800 V on the Ag anode. In the first step of the discharge the accelerated electrons heat the materials until melting and a stable inter-electrode metallic vapor pressure is achieved. In the second step by increasing the anode voltage a localized plasma is ignited in the metallic vapors of both Cu and Ag, with discharge currents of 0.9 A for the first one and 0.7 A for the second. During the deposition the substrates were electrically grounded and were radiatively heated by both plasma sources reaching a maximum temperature of 100 °C.

For each material-of-interest films, deposition rate and thickness respectively were in situ monitored using a quartz-micro balances (QMB) placed above each crucible. Both devices were shielded from each other in order to measure only the particle flow coming from the anode over which these are positioned. The QMB probes were connected to a film thickness monitoring device (FTM) which in turn was connected to the computer.

The center of the sample holder was positioned at a distance of 27 cm from the Ag containing crucible respectively 32.5 cm from Cu crucible. Because of the longitudinal positioning of the substrates in fixed deposition geometry, it is expected to obtain variable concentrations of both materials used, depending on the distance between the samples and place of evaporation. The total deposition rate for all performed coatings was maintained with approximation at a value of 0.4 nm/s.

2.2. Morphological, Structural, and Compositional Analysis of Cu-Ag Thin Layers

SEM measurements were performed on Cu-Ag thin films deposited on stainless steel substrates. For this purpose, a FEI Co. Model Inspect S (Hillsboro, OR, USA). was used. SEM images were taken using a 25 kV acceleration voltage at a working distance of 13.5 mm, working pressure 7.5×10^{-7} torr, and different magnifications 1000 \times , 5000 \times , and 20000 \times . Atomic force microscopy (AFM) measurements were carried out with a Park XE-100 model (Park Systems, Suwon, Korea) in contactless operation mode using a silicon cantilever with a nominal length of 125 μ m and oscillation range between 275 and 328 kHz on a $5 \times 5 \mu$ m scanned surface. The average root mean square (RMS) roughness was calculated by means of image processing software.

Crystalline structure of Cu-Ag thin films deposited on silicon substrates was investigated by means of X-ray diffraction (XRD). These measurements were carried out using a Bruker D8 Advance diffractometer (Coventry, West Midlands, UK). A Bragg–Bretano configuration was used in 2θ range between 20° and 80° with a step size of 0.01° and 2 s integration time per step.

The atomic ratio of the obtained composite coatings on the grids was analyzed using low value excitation energies (<50 keV) by the method named (μ -XRF). This method can focus the X-ray beam on a small surface area (500 μ m² with a beam spot diameter of 25 μ m) of the sample using a polycapillary lens.

Rutherford backscattering spectrometry (RBS) was applied to analyze the elemental depth profile and thickness for Cu-Ag (65–35 at.%) sample. The experimental set-up involved bombarding the sample with a monoenergetic 3.7 MeV double ionized He beam (1 mm diameter) and analyzing the energies of the backscattered particles. The depth profile was determined by simulating the experimental spectra with SIMRA code.

Sliding wear behavior of the Cu-Ag coatings was provided using a Ball-on-Disk CMS Tribometer (CSM instruments, Needham city, MA, USA). This study was performed by sliding the Cu-Ag coated stainless steel disks against a stainless steel stationary sphere at normal loading force of 1 N, 2 N, 3 N respectively 5 N, 100 m sliding distance using a constant linear speed of 2 cm/s.

2.3. Antibacterial Properties Evaluation

The antibacterial testing of the Cu-Ag coated stainless-steel grids consisted of two separate experiments. The first experiment was designed to pass *S. aureus* contaminated air through the grids in order to determine which Cu/Ag ratio has the highest bacterial retention efficiency. The setup for the first experiment is presented in Figure 2a. To perform this experiment, skin samples were collected in order to isolate a strain of *Staphylococcus aureus*. The skin samples were provided with informed consent of the individual donors, in full respect with the Declaration of Helsinki. We used a general culture medium that allows the development of a variety of microorganisms. Sabouraud culture medium, which consists of the following compounds: peptone- 10 g; glucose- 20 g; agar- 20 g; distilled water- 1000 mL, was sterilized, dispensed into petri dishes, and seeded with biological samples of skin derived from various subjects. After sowing, the Petri dishes were incubated at 37 °C for 48 h for the microorganisms to grow. Most boards achieved mixed cultures, but *S. aureus* cultures were predominant. The next step was isolating pure culture of *S. aureus* strain on tryptase soy broth (TSB) medium containing (g/l): bacto tryptone, 17 g; bactosoytone, 3 g; glucose, 2.5 g; NaCl, 5 g; K₂HPO₄, 2.5 g; agar, 20 g; pH, 7.3 ± 0.2. The isolated *S. aureus* strain was characterized by macroscopic, microscopic, and biochemical analyses to determine its coagulation properties. Isolated in pure culture and identified, *S. aureus* was used in experiments to determine the effectiveness of the antibacterial grids.

For testing, Cu-Ag films were deposited on the two dimensioned grids (1 × 1 mm² and 0.5 × 0.5 mm²).

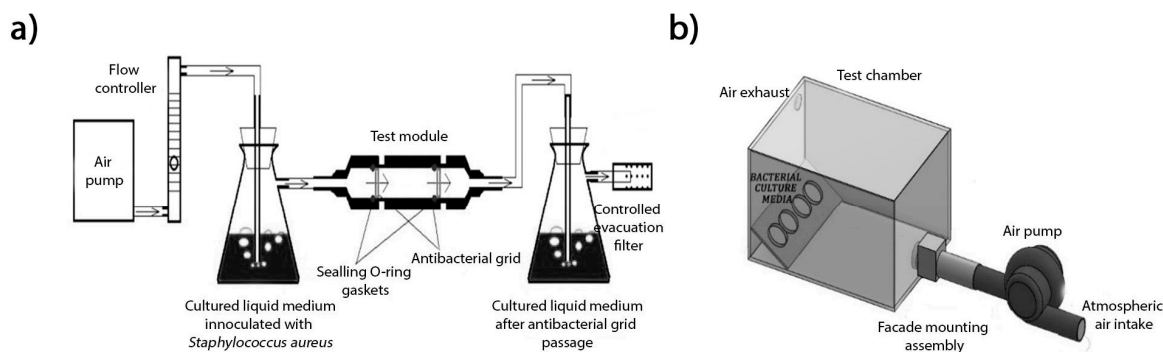


Figure 2. Experimental setup for testing: (a) Cu-Ag grids antibacterial properties; (b) air quality improvement with Cu-Ag grids.

The grids were mounted inside a specially designed device that forces air contaminated with bacteria through them. A compressor pushes air, with a flux of 0.2 l/s into a cultured liquid medium inoculated with a strain of *S. aureus* and by means of bubbling, the bacteria is picked up by the air flow and passed through the grids. The bacteria that passed were collected into a cultured liquid medium (TSB agar). *Staphylococcus aureus* culture maintained in TSB agar was activated by inoculation in liquid TSB medium (250 mL). The development was performed for 18 h under aeration and agitation using an Orbital Shaker 3005.

After the results of the first *S. Aureus* contaminated air experiment the coating which showed the best antibacterial properties was subsequently tested in a second experiment under normal working conditions. In order to test the air quality improvement by means of filtering the outdoors air through Cu-Ag grids a test chamber (Figure 2b) was designed to replicate the normal operation of an SVS module. This experiment was designed to test antibacterial behavior for prolonged exposure by

introducing large volumes of air through the grids. The atmospheric air is pumped inside the reaction chamber passing through the filtering system and because of admission-evacuation system it creates air currents inside the chamber, which in turn facilitate the trapping of the remaining pathogens in the bacterial culture media. For this study four different types of bacteria culture media were used to follow microbiological markers corresponding to *Escherichia coli*, *Staphylococcus aureus*, *Pseudomonas aeruginosa*, and air microbiota (microfungi, bacterias).

3. Results and Discussion

3.1. Bactericidal Efficiency and Air Quality Improvement

Removal efficiency of microorganisms was measured by sampling the liquid cultured medium, after *S. Aureus* contaminated air was passed through the investigated grids for 60 min. After sampling, serial dilutions were performed and the TSB agar distributed in Petri plates was seeded with 1 mL diluted liquid cultured medium suspension. Seeded Petri plates were then incubated at 37 °C for the growth of microorganisms. The results are expressed in colony forming units per ml (CFU/mL). It is important to mention that decontamination procedures were performed before and after each experimental variation in order to not influence the results. The background results indicated that without a grid the culture medium is heavily inoculated with *S. aureus* and we were not able to read the results because of the fact that the Petri dish is covered with a continuous biofilm of *S. aureus* and no individual CFU can be distinguished.

So, the retention efficiency of the coated grids is calculated in relation to the uncoated grids, using the following formula:

$$R_{\text{efficiency}} = [1 - (\text{CFU}_{\text{coated grid}}/\text{CFU}_{\text{uncoated grid}})] \times 100\%$$

The first reference measurements were performed on uncoated grids with pore dimension of $1 \times 1 \text{ mm}^2$ respectively $0.5 \times 0.5 \text{ mm}^2$. It was observed that pore dimension also influences bacteria retention. For example, $0.5 \times 0.5 \text{ mm}^2$ grids have 33% higher bacterial retention efficiency than $1 \times 1 \text{ mm}^2$ grids.

The graph above shows a clear effect that the coated grids have on bacteria trapping and killing. It is highlighted that the Cu-Ag layers show a high antibacterial activity for $1 \times 1 \text{ mm}^2$, reducing to half the total number of CFU. The trapping and killing of bacteria are highly enhanced for the fine pore Cu-Ag-coated grids. It is highlighted that the bacteria retention is 15–18 times higher than in the case of coarse coated grids with a total retention over 90% which varies with the Cu/Ag ratio deposited. It was observed that in the case of Cu-Ag (65%–35%) the retention of *S. aureus* CFU was 100%. As it can be observed in Figure 3, atomic composition of Cu-Ag layers represents a major factor in regard to the antibacterial activity. We cannot distinguish from our measurements between the number of CFU that are killed in contact with the thin films and the ones that only adhered to the surface of the grids. But one can assume that the latter is negligible, considering the bacteria dimensions (several micrometres) and the grid pores size. However, considering the high level of filtering (100%) one cannot exclude the probability that the bioaerosol liquid particles, formed from bubbling the liquid culture medium, carry the *S. aureus* condense on metallic Cu-Ag coated mesh leading to contact killing. The results showed better antibacterial properties for the coatings with a higher Cu content in composition. This may be related to the diffusivity of the Cu ions from the surface through the bacteria membrane cell which ultimately results in its killing. This theory received support in a number of different studies [23–25].

Since the best results were obtained for Cu-Ag (65–35 at.%), this type of coatings was also used for air filtration measurements. The obtained results for each experimental variation are highlighted in Table 2. It is important to specify that physical parameters like temperature and relative humidity may influence the diversity and number of bacteria in the outdoor air during the experiments.

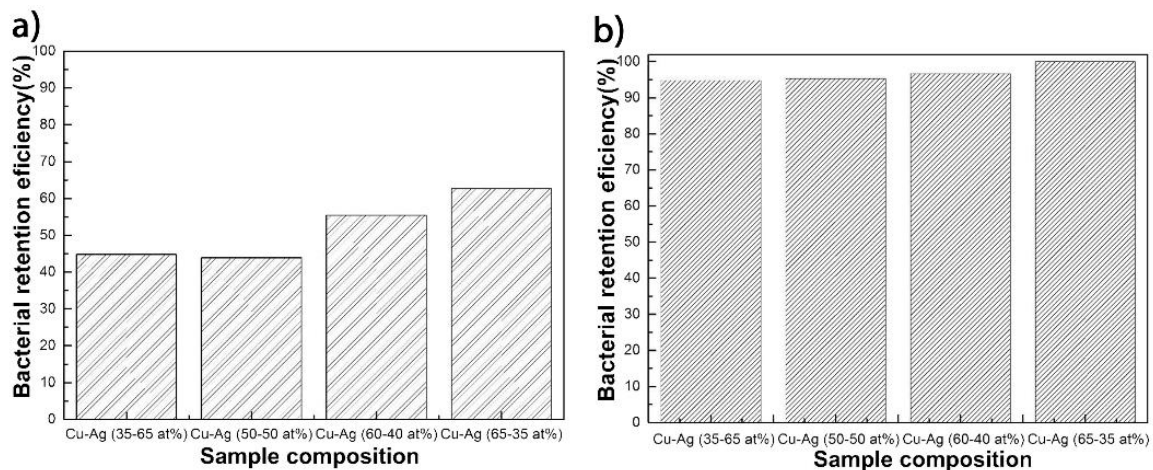


Figure 3. Bacterial retention efficiency measured after 60 min exposure to *S. aureus*-contaminated air for: a) 1 × 1 mm Cu-Ag coated grids; b) 0.5 × 0.5 mm Cu-Ag coated grids.

Table 2. Air filtration measurement result for tested microbiological markers.

Nr.	Experimental Setup	Exposure Time (h)	Microbiological Markers (CFUa)			
			Microbiota	<i>E. coli</i>	<i>P. aeruginosa</i>	<i>S. aureus</i>
1	Background measurement	1	20	1	2	1
		3	Microfungi	4	0	0
2	Uncoated grid 1 × 1 mm ²	1	13	4	0	0
		3	19	3	0	0
3	Uncoated grid 0.5 × 0.5 mm ²	1	6	1	0	0
		3	5	1	0	0
4	Cu-Ag (65–35 at.%) coated grid 1 × 1 mm ²	1	1	0	0	0
		3	1	0	0	0
5	Cu-Ag (65–35 at.%) coated grid 0.5 × 0.5 mm ²	1	0	0	0	0
		3	1	0	0	0

As it was seen from Table 2 the most relevant microbiological marker for this experiment is the total microbiota. In the case of the other three markers the background measurements reveal a low number of characteristic bacteria colonies. Background measurements for total microbiota show a number of 20 CFU after 1 h and after 3 h the entire surface of bacteria growing media was covered with microfungi. For 1 × 1 mm² uncoated grid the total CFU characteristic for microbiota was 13 colonies after 1 h and 19 colonies after 3 h, respectively. For the other markers only in the case of *E. Coli*, 3 and 4 CFU were recorded after 1 h and 4 h respectively. The results obtained for 0.5 × 0.5 mm² uncoated grids show a decreasing number of the microbiota CFU with 54% after 1 h and 74% after 3 h in comparison to results obtained for 1 × 1 mm² uncoated grid. No characteristic colonies were observed for the other three markers except for *E. Coli*. The fourth measurement was conducted using a Cu/Ag 1 × 1 mm² coated grid. The recorded data show a sharp decrease in the number of specific colonies compared to the uncoated grid. The bacteria retention in this case was over 90%.

Results obtained for 0.5 × 0.5 mm² Cu-Ag coated grid show a total retention for microbiota after 1 h of air filtering and after 3 h only one specific colony was observed. Also, no CFU were observed for the other three microbiological markers. This clearly shows how effective this type of coated grids are, which makes them suitable to be employed as SVS bacterial filtering systems. Although the bactericidal effect of the layer was not directly evidenced, a similar study performed on air filters with silver nanoclusters embedded in a silica matrix highlights a 100% reduction of Gram-positive *S. epidermidis* and Gram-negative *E. coli* on the coated filter after bacterial contamination tests [26].

3.2. Atomic Composition and Depth Profile

μ -XRF results obtained for the set of Cu-Ag thin films deposited in fixed geometry show an evolution of Cu and Ag atomic ratio in layers as a function of substrate position (Figure 4b). The X-axis represents the sample index, where 3.1 is the stainless steel grid placed directly above the Ag plasma, 3.12 above the Cu plasma source, and 3.6 is placed at an equal distance from both sources. This is due to the longitudinal distribution of the substrates between Cu anode and Ag anode during the deposition process. A decrease is observed in the atomic concentration of Ag from 70% for the sample placed in the proximity of Ag plasma source to 10% for those positioned above the Cu plasma source. The evolution of Cu atomic concentration in layers was complementary to Ag concentration. Since equal mixing for both elements were not achieved for SAMPLE 3.6 it implies that in situ Cu particle flux from plasma was higher than for Ag. This was useful in order to obtain a wide range of atomic concentration in the Cu-Ag layers with the aim to determine the optimum composition with a maximum efficiency for trapping and killing bacteria.

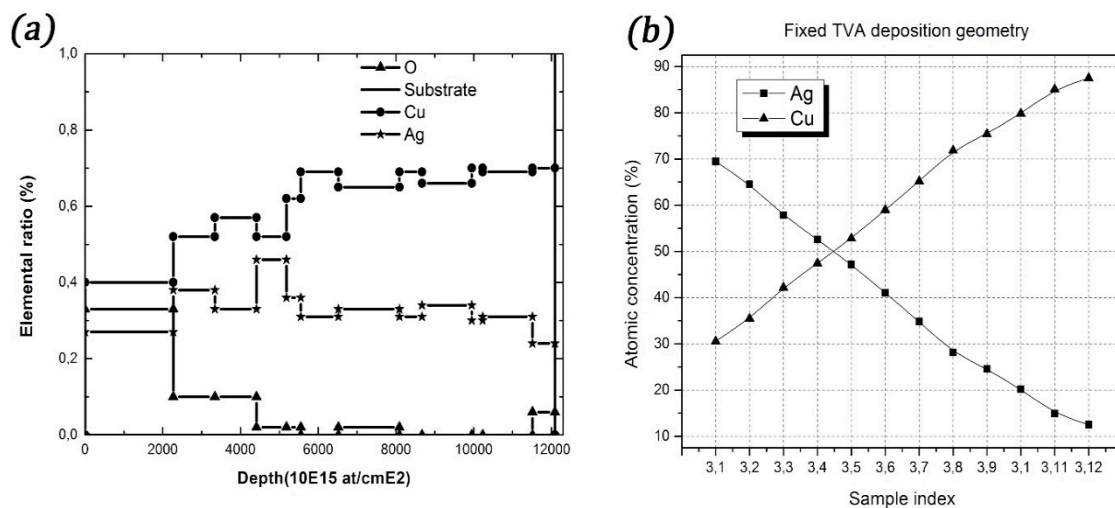


Figure 4. (a) Rutherford backscattering spectrometry (RBS) depth profile of Cu-Ag (65–35 at%); (b) μ -XRF results of Cu-Ag samples deposited in fixed geometry.

The RBS depth profiles for Cu-Ag (65–35 at.%) presented in Figure 4a indicate a variation of concentrations in film depth that could be most likely determined either by fluctuations of the deposition parameters during the coating process or because of low method resolution for thick coatings. A high oxygen contamination (35 at.%) is observed in the surface layers. The presence of oxygen in the surface layers is caused by the oxidation in open atmosphere after the deposition process. Also, a small oxygen content (6–8 at.%) is observed at film-substrate interface most likely caused by oxygen impurities from Cu and Ag anodes at the beginning of the coating process.

3.3. Surface Morphology

Bacteria interaction with Cu-Ag solid surfaces are governed by long and medium range forces, in particular by Van der Waals and electrostatic force [27,28]. Thus, surface morphology and composition have a decisive role in trapping and neutralizing bacteria [29]. SEM images (Figure 5a–c) show the textured nature of the surface composed of Cu and Ag structures without a well-defined shape but evenly distributed along the surface.

SEM and AFM images revealed an irregular shaped surface. In order to analyze the average surface roughness three random scanning areas $5 \times 5 \mu\text{m}^2$ (Figure 5d) were selected. The mean value for RMS roughness of Cu-Ag thin films was $500 \text{ nm} \pm 50 \text{ nm}$.

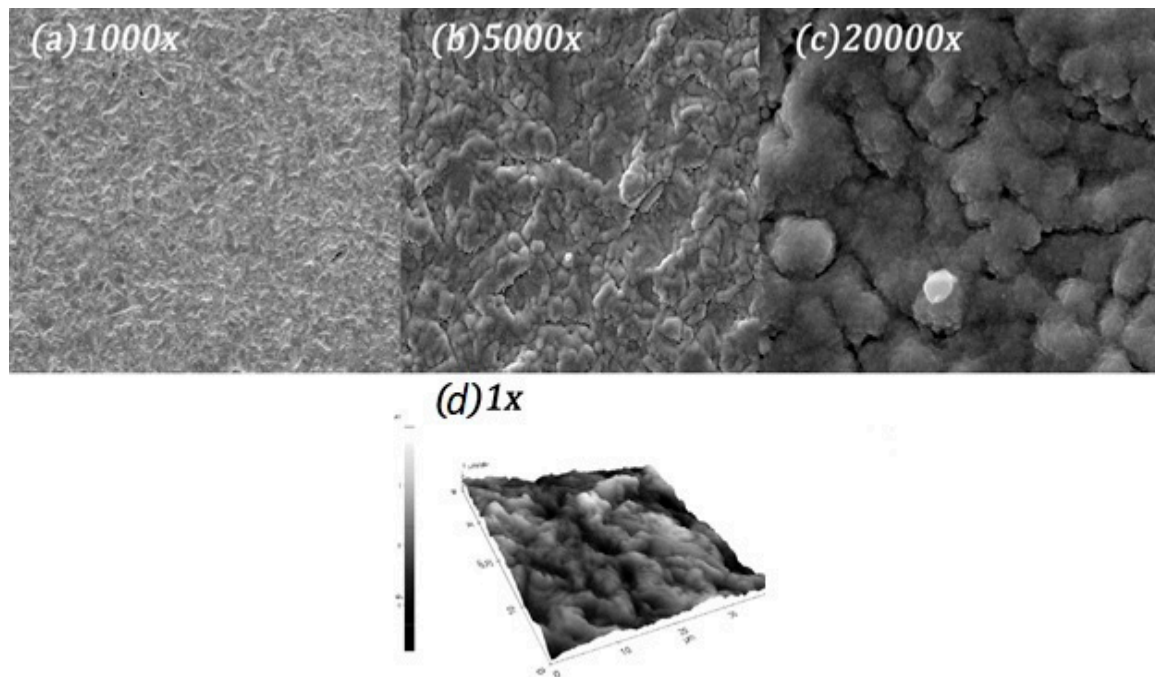


Figure 5. SEM images of Cu-Ag (65%–35%) thin layers deposited on stainless steel disks at different magnifications: (a) 1000 \times ; (b) 5000 \times ; (c) 20000 \times ; and (d) AFM image of the layer surface

Moreover, the hydrophilicity of the Cu-Ag (65%–35%) sample was determined using distilled water. The contact angle measurement results revealed an increase in the surface contact angle to $122^\circ \pm 0.2^\circ$ for the Cu-Ag layers compared to stainless surface that had a measured value of $70^\circ \pm 0.2^\circ$. In this context the hydrophobicity of the Cu-Ag layers facilitates bacteria adhesion in comparison to stainless steel surfaces [30]. This increase, and the high surfaces roughness represent positive characteristics due to the facts that the layers have a better adhesion for humid particles and an increased contact surface for trapping and killing bacteria.

3.4. Structural Characterization

X-ray diffraction pattern in Figure 6 reveals the crystalline structure of Cu-Ag thin films by the presence of a two-phase metallic structure corresponding to Cu, Fm-3m spatial group with a face-centered cubic arrangement of atoms, Ag, spatial group Fm-3m and the same atom arrangement as in the case of Cu, respectively. These structures were identified by the crystalline growth on Ag 111, Ag 220, Ag 311, Ag 220 and Cu 111, Cu 110, Cu 200, Cu 220. Both Cu and Ag exhibit preferential crystalline growth on 111 orientation. The Ag average grain size dimension was evaluated from Ag 111 FWHM using Scherrer equation. The obtained value for crystallite size was 20.9 nm with a lattice strain of 0.005. The calculated Cu average grain size was around 14.1 nm with a lattice strain of 0.006. It was concluded from comparison between peak intensities that the dominant crystalline structure corresponds to metallic Ag.

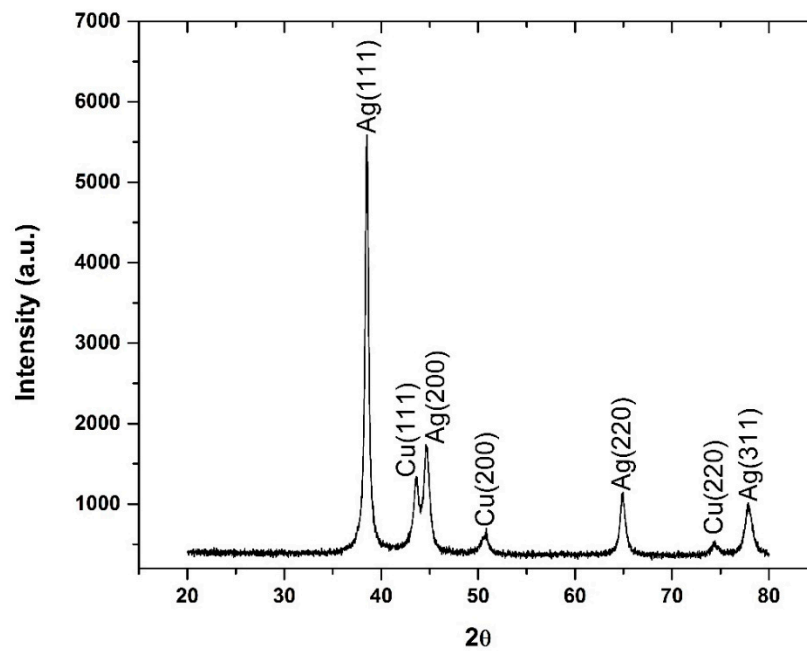


Figure 6. X-ray diffraction pattern for Cu-Ag thin films deposited on silicon substrate.

3.5. Sliding Wear Behavior of Cu-Ag Thin Films

Since Cu-Ag (65–35 at.%) layers showed the best antibacterial properties as can be seen in the antibacterial testing Section 3.1 of this study, tribo-measurements were also performed on these samples deposited on stainless steel substrates in order to assess the wear mechanisms of the coated grids used for SVS. SEM images were taken on an area of the wear tracks at 1000× magnification for each experimental variation. The main purpose was to identify the main wear mechanism responsible for surface erosion. Images in Figure 7 represent an evolution of the erosion markers under increasing applied normal force.

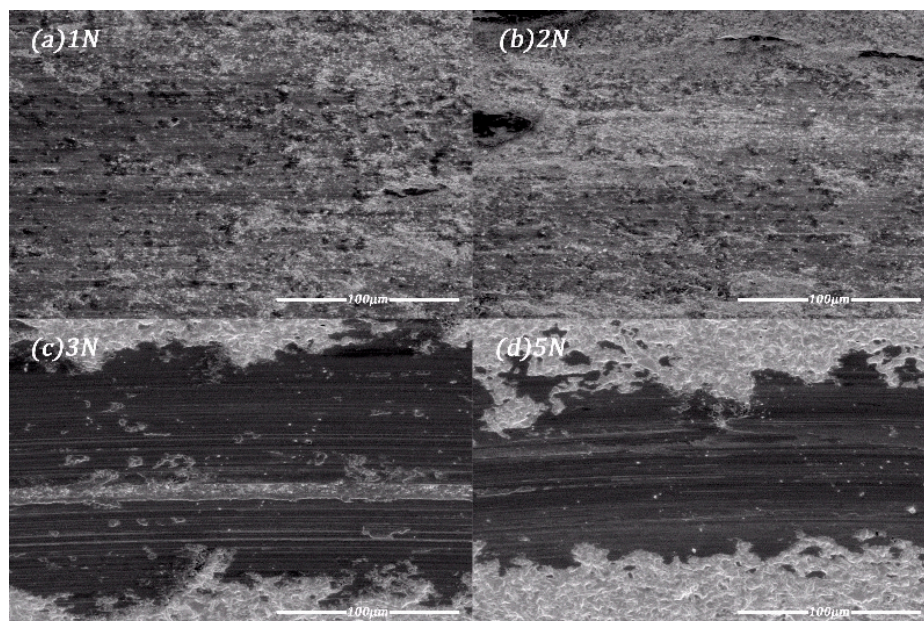


Figure 7. SEM Images of an area in the wear track for different normal load forces: (a) 1N; (b) 2N; (c) 3N; (d) 5N.

Figure 7a,b show an area of the wear tracks for 1N and 2N normal load. They both exhibit extensive plastic deformations of the coating surface produced by the plowing action of the stainless-steel counter material. The occurrence of plastic deformation is highlighted furthermore by a close observation of parallel tears along the wear track, visible especially at 1N normal load. Also, isolated micro-fracture areas can be observed on the wear track at 2N normal load force. For 3N and 5N load force the coating surface is completely removed from the substrate after a sliding distance of 50 m (Figure 7c), 40 m (Figure 7d) respectively with the exception of an area along the wear track (Figure 7c) due to debris accumulated on the stainless-steel ball. This furthermore is an indication that adhesion has occurred between the coating surface and counter material during the sliding experiment. Coating adherence to the substrate greatly influences the lifetime of the coated grids. The investigated coating exhibit very good adherence to substrate and the main wear mechanism responsible for delamination is shearing by a harder material [31].

4. Conclusions

The stainless-steel grids used for air filtering in an SVS prototype currently built in our laboratory were successfully coated with Cu-Ag layers with various concentrations using TVA plasma processing technology. The air filtration properties were investigated by passing an air flow contaminated with *S. aureus* through the Cu-Ag coated grids. The results showed that grids pore dimension influences the bacterial retention efficiency, indicating a 33% increase for 0.5 mm × 0.5 mm pore grids compared to 1 × 1 mm grid. In terms of coating influence, the best results were obtained for Cu-Ag (65%–35%) for both types of porous grids, showing an increase of 65% compared to the uncoated 1 × 1 mm grid and total retention 100% for the 0.5 × 0.5 mm. The second experimental setup for atmospheric air filtration experiment performed only on reference and Cu-Ag (65%–35%) coated grids confirms the efficiency of the coated grids showing a total reduction in CFU for the only relevant biological marker (microbiota). The morphological, structural, and compositional measurements were performed only on the coating which showed the best antibacterial activity, namely Cu-Ag (65%–35%). The layers' increased surface roughness and hydrophobicity favour bacteria adhesion which leads to a high retention of pathogenic agents. Crystalline structure of the investigated layers revealed two separate highly oriented metallic phases corresponding to Cu and Ag. Mechanical wear measurements highlight a very good adherence of the layers to the stainless-steel substrate and also good wear resistance properties. The positive results obtained in this study confirms that simple metallic grids coated with Cu-Ag can help in overcoming the weakness of the natural ventilation systems in terms of outdoor air filtering, thus reducing the microorganism concentration in indoor air.

Author Contributions: Investigation: M.L., I.J., P.D., C.S., A.N., I.B., B.B., O.T., M.D., I.C., G.S.; Methodology: P.D. and C.P.; Project administration: C.P.; Supervision: C.P.L.; Writing—original draft P.D. All authors have read and agreed to the published version of the manuscript.

Funding: This work was supported by a grant of the Romanian National Authority for Scientific Research—ANCS, Core Program—contract number: “LAPLAS VI, 16N/2019” and project number 80/2014, PN-II-PT-PCCA-2013-4-2165.

Conflicts of Interest: The authors declare no conflict of interest. The funders had no role in the design of the study; in the collection, analyses, or interpretation of data; in the writing of the manuscript, or in the decision to publish the results.

References

1. Miaškiewicz-Peska, E.; Łebkowska, M. Effect of antimicrobial air filter treatment on bacterial survival. *Fibres. Text. East. Eur.* **2011**, *19*, 73–77.
2. Payne, S.C.; Benninger, M.S. Benninger, Staphylococcus aureus is a Major Pathogen in Acute Bacterial Rhinosinusitis: A Meta-Analysis. *Clin. Infect. Dis.* **2007**, *45*, 121–127. [[CrossRef](#)]

3. Durupt, F.; Mayor, L.; Bes, M.; Reverdy, M.E.; Vandenesch, F.; Thomas, L. JEtienne Prevalence of Staphylococcus aureus toxins and nasal carriage in furuncles and impetigo. *Br. J. Dermatol.* **2007**, *157*, 1161–1167. [[CrossRef](#)] [[PubMed](#)]
4. Gorwitz, R.J. A Review of Community-Associated Methicillin-Resistant Staphylococcus aureus Skin and Soft Tissue Infections. *Pediatr. Infect. Dis.* **2008**, *27*, 1–7. [[CrossRef](#)] [[PubMed](#)]
5. Liu, G.Y. Molecular Pathogenesis of Staphylococcus aureus. *Infect. Pediatr. Res.* **2009**, *65*, 71–77. [[CrossRef](#)] [[PubMed](#)]
6. Wertheim, H.F.; Melles, D.C.; Vos, M.C.; van Leeuwen, W.; van Belkum, A.; Verbrugh, H.A.; Nouwen, J.L. The role of nasal carriage in Staphylococcus aureus infections. *Lancet Infect. Dis.* **2005**, *5*, 751–762. [[CrossRef](#)]
7. Lowy, F.D. Staphylococcus aureus infections. *N. Engl. J. Med.* **1998**, *339*, 520–532. [[CrossRef](#)]
8. Gordon, R.J.; Lowy, F.D. Pathogenesis of methicillin-resistant Staphylococcus aureus infection. *Clin. Infect. Dis.* **2008**, *46*, S350–S359. [[CrossRef](#)]
9. van Belkum, A.; Emonts, M.; Wertheim, H.; de Jongh, C.; Nouwen, J.; Bartels, H.; Cole, A.; Hermans, P.; Boelens, H.; Toom, N.L.; et al. The role of human innate immune factors in nasal colonization by Staphylococcus aureus. *Microbes. Infect.* **2007**, *9*, 1471–1477. [[CrossRef](#)]
10. Kawada-Matsuo, M.; Komatsuzawa, H. Factors affecting susceptibility of Staphylococcus aureus to antibacterial agents. *J. Oral Biosci.* **2012**, *54*, 86–91. [[CrossRef](#)]
11. Wertheim, H.F.; Vos, M.C.; Ott, A.; van Belkum, A.; Voss, A.; Kluytmans, J.A.; van Keulen, P.H.; Vandembroucke-Grauls, C.M.; Meester, M.H.; Verbrugh, H.A. Risk and outcome of nosocomial Staphylococcus aureus bacteraemia in nasal carriers versus non-carriers. *Lancet* **2004**, *364*, 703–705. [[CrossRef](#)]
12. Rooijackers, S.H.; van Kessel, K.P.; van Strijp, J.A. Staphylococcal innate immune evasion. *Trends Microbiol.* **2005**, *13*, 596–601. [[CrossRef](#)] [[PubMed](#)]
13. McLean, R.J.; Hussain, A.A.; Sayer, M.; Vincent, P.J.; Hughes, D.J.; Smith, T.J. Antibacterial activity of multilayer silver–copper surface films on catheter material. *Can. J. Microbiol.* **1993**, *39*, 895–899. [[CrossRef](#)] [[PubMed](#)]
14. Ren, G.; Hu, D.; Cheng, E.W.; Vargas-Reus, M.A.; Reip, P.; Allaker, R.P. Characterisation of copper oxide nanoparticles for antimicrobial applications. *Int. J. Antimicrob. Agents* **2009**, *33*, 587–590. [[CrossRef](#)] [[PubMed](#)]
15. Santo, C.E.; Morais, P.V.; Grass, G. Isolation and characterization of bacteria resistant to metallic Copper surfaces. *Appl. Environ. Microbiol.* **2010**, *76*, 1341–1348. [[CrossRef](#)]
16. Jung, J.; Hwang, G.; Lee, J.; Bae, G. Preparation of airborne Ag/CNT hybrid nanoparticles using an aerosol process and their application to antimicrobial air filtration. *Langmuir* **2011**, *27*, 10256–10264. [[CrossRef](#)]
17. Brobbey, K.; Haapanen, J.; Gunell, M.; Mäkelä, J.; Eerola, E.; Toivakka, M.; Saarinen, J. One-step flame synthesis of silver nanoparticles for roll-to-roll production of antibacterial paper. *Appl. Surf. Sci.* **2017**, *420*, 558–565. [[CrossRef](#)]
18. Hassan, I.; Parkin, I.; Nair, S.; Carmalt, C. 2014 Antimicrobial activity if copper and copperI oxide thin films deposited via aerosol-assisted CVD. *J. Mater. Chem. B* **2014**, *2*, 2855. [[CrossRef](#)]
19. Lungu, C.P.; Mustata, I.; Musa, G.; Lungu, A.M.; Zaroschi, V.; Iwasaki, K.; Tanaka, R.; Matsumura, Y.; Iwanaga, I.; Tanaka, H.; et al. Formation of nanostructured Re–Cr–Ni diffusion barrier coatings on Nb superalloys by TVA method. *Fujita Surf. Coat. Technol.* **2005**, *200*, 399. [[CrossRef](#)]
20. Lungu, C.P.; Mustata, I.; Zaroschi, V.; Lungu, A.M.; Anghel, A.; Chiru, P.; Rubel, M.; Coad, P.; Matthews, G.F. JET-EFDA contributors. Beryllium Coatings on Metals: Development of Process and Characterizations of Layers. *Phys. Scr. T* **2007**, *128*, 157. [[CrossRef](#)]
21. Surdu-Bob, C.; Mustata, I.; Iacob, C. General characteristics of the Thermoionic Vacuum Arc plasma. *J. Optoelectron. Adv. Mater.* **2007**, *9*, 2932–2934.
22. Lungu, C.P.; Mustata, I.; Musa, G.; Lungu, A.M.; Brinza, O.; Moldovan, C.; Rotaru, C.; Iosub, R.; Sava, F.; Popescu, M.; et al. Unstressed carbon-metal films deposited by thermionic vacuum arc method. *J. Optoelectron. Adv. Mater.* **2006**, *8*, 74–77.
23. Santo, C.E.; Lam, E.W.; Elowsky, C.G.; Quaranta, D.; Domaille, D.W.; Chang, C.J.; Grass, G. Antimicrobial metallic copper surfaces kill Staphylococcus haemolyticus via membrane damage. *Appl. Environ. Microbiol.* **2011**, *77*, 794–802. [[CrossRef](#)] [[PubMed](#)]
24. Molteni, C.; Abicht, H.K.; Solioz, M. Killing of bacteria by copper surfaces involves dissolved copper. *Appl. Environ. Microbiol.* **2010**, *76*, 4099–4101. [[CrossRef](#)]

25. Ibrahim, M.; Wang, F.; Lou, M.M.; Xie, G.L.; Li, B.; Bo, Z.; Zhang, G.Q.; Liu, H.; Wareth, A. Copper as an antibacterial agent for human pathogenic multidrug resistant Burkholderia cepacia complex bacteria. *J. Biosci. Bioeng.* **2011**, *112*, 570–576. [[CrossRef](#)]
26. Balagna, C.; Perero, S.; Bosco, F.; Mollea, C.; Irfan, M.; Ferraris, M. Antipathogen nanostructured coating for air filters. *Appl. Surf. Sci.* **2020**, *508*, 145283. [[CrossRef](#)]
27. Fletcher, M. *Bacterial Adhesion: Molecular and Ecological Diversity*; Wiley–Liss: New York, NY, USA, 1996; pp. 1–24.
28. Razatos, A.; Ong, Y.; Sharma, M.M.; Georgious, G. Molecular determinants of bacterial adhesion monitored by atomic force microscopy. *Proc. Natl. Acad. Sci. USA* **1998**, *95*, 11059–11064. [[CrossRef](#)]
29. Nan, L.; Liu, Y.; Lu, M.; Yang, K. Study on antibacterial mechanism of copper-bearing austenitic antibacterial stainless steel by atomic force microscopy. *J. Mater. Sci. Mater. Med.* **2008**, *19*, 3057–3062. [[CrossRef](#)]
30. Dou, X.; Zhang, D.; Feng, C.; Jiang, L. Bioinspired Hierarchical Surface Structures with Tunable Wettability for Regulating Bacteria Adhesion. *ACS Nano* **2015**, *9*, 10664–10672. [[CrossRef](#)]
31. Panagopoulos, C.N.; Georganakis, K.G.; Petroutzakou, S. Sliding wear behaviour of zinc–cobalt alloy electrodeposits. *J. Mater. Process. Technol.* **2005**, *160*, 234–244. [[CrossRef](#)]



© 2020 by the authors. Licensee MDPI, Basel, Switzerland. This article is an open access article distributed under the terms and conditions of the Creative Commons Attribution (CC BY) license (<http://creativecommons.org/licenses/by/4.0/>).